International Journal of Nanomedicine

Dovepress
open access to scientific and medical research

Open Access Full Text Article

ORIGINAL RESEARCH

Ultralow-intensity NIR light triggered on-demand drug release by employing highly emissive UCNP and photocleavable linker with low bond dissociation energy

This article was published in the following Dove Press journal:
International Journal of Nanomedicine

Junhui Shi[1]
Zhengyan Zhao[2]
Zongjun Liu[3]
Ruozheng Wu[1]
You Wang[1]

[1]School of Materials Science and Engineering, Harbin Institute of Technology, Harbin 150001, People's Republic of China; [2]State Key Laboratory of Fine Chemicals, Dalian University of Technology, Dalian 116024, People's Republic of China; [3]School of Chemistry and Chemical Engineering, Harbin Institute of Technology, Harbin 150001, People's Republic of China

Background: The design of novel nanoparticles with higher therapeutic efficacy and lower side effects, is still difficult but encouraging in cancer therapy. Specifically, for upconversion nanoparticles (UCNP)-based drug release, a high intensity of NIR light (1.4~5.0 W/cm^2) above the maximum permissible exposure (0.33 W/cm^2 for 980 nm) is commonly used and severely limits its practical application.

Methods: The highly emissive UCNP is first synthesized and then coated with mesoporous silica (MS) shell (UCMS). Next, the surface of UCMS is modified with the thioether (-S-BP) linker, leading to UCMS-S-BP nanoparticles. Finally, after the drug doxorubicin (Dox) is loaded into the pore channels of UCMS, the pore openings are blocked by the β-cyclodextrin (β-CD) gatekeeper through the association with the -S-BP linker (UCMS(Dox)-S-BP@β-CD).

Results: Upon 980 nm NIR light irradiation with an ultralow intensity of 0.30 W/cm^2, it is found that the loaded Dox can be released through the cleavage of thioether linkers triggering dissociation of β-CD gatekeepers. The in vitro results exhibited significantly therapeutic efficacy with 85.2% of HeLa cells killed in this study.

Conclusions: An ultralow-intensity NIR light triggered on-demand drug release system has been developed by employing highly emissive UCNP and photocleavable linker with low bond dissociation energy to avoid the potential photodamage on healthy neighbor cells.

Keywords: drug release, ultralow intensity, density functional theory, near infrared light, upconversion nanoparticles

Introduction

Chemotherapy (Chemo) is an important/extensive method applied nowadays in clinical cancer therapy. The success of Chemo requires the precise delivery of anticancer drugs to cancerous cells and to avoid the killing of normal cells.[1,2] Therefore, various drug releases based on such stimuli as pH,[3,4] ultrasonic,[5] light,[6,7] and glutathione[8,9] have been developed. Among these stimuli, light exhibits obvious advantages over the others, which can afford drug release both spatially and temporally, owning to its excellent merits of input intensity and tunable wavelength.[10,11] Initially, either ultraviolet (UV) and visible (Vis) light was used to trigger drug release.[7] However, the high energy UV/Vis lights can cause DNA damage and living cell death. Furthermore, they are widely absorbed by tissue, which diminishes their

Correspondence: You Wang
Materials Physics and Chemistry Department, School of Materials Science and Engineering, Harbin Institute of Technology, Harbin 150001, People's Republic of China
Tel +864 518 641 2516
Fax +864 518 641 2516
Email y-wang@hit.edu.cn

submit your manuscript | www.dovepress.com
DovePress
http://doi.org/10.2147/IJN.S201982

penetration depth to a few microns, thus limiting their potential use in practical application. Compared to UV/Vis light, near-infrared (NIR) light (700~1100 nm) is at the biological window with significantly deeper tissue penetration, weak background fluorescence, and a negligible irradiation damage.[12] Unfortunately, unlike UV/Vis lights, the energy of NIR light is insufficient to trigger a photochemical reaction, on which drug release is based.[13]

Upconverting nanoparticles (UCNP),[14] which can absorb NIR light and convert it into high energy UV or Vis lights, have therefore been employed as photo-transducers to open the door for the development of NIR-based drug release.[15] For example, Cui et al[13] reported a NIR-triggered drug release based on mesoporous silica (MS)-coated UCNP (UCMS) with *o*-nitrobenzyl used as photolabile linker upon 1.4 W/cm^2 of 980 nm NIR light irradiation Liu et al[16] also reported a photo-responsive drug delivery based on UCMS nanoplatform, where the anticancer drug doxorubicin (Dox) was released by the isomerization of azobenzene molecule upon 2.4 W/cm^2 intensity NIR light irradiation. However, relatively high NIR laser intensities ranging from 1.4 to 5.0 W/cm^2, which is well above the maximum permissible exposure (MPE) of skin (0.33 W/cm^2, 980 nm laser)[24] according to the American National Standard for Safe Use of Lasers, have been popularly used for the NIR-responsive drug release[13,16–23] (see Table S1). The employed high intensity of NIR light irradiation well above MPE will certainly lead to overheating and/or photodamage of skin,[24] which should be a fundamental challenge for the NIR-responsive chemotherapy. In a pioneering work to address the challenge, He et al[22] recently reported NIR-induced drug release at an ultralow intensity of 0.35 W/cm^2. Few studies have been reported so far to the best of our knowledge.

To enable drug release to be triggered upon NIR light irradiation at an ultralow-intensity below MPE, in this work we first prepared one of the most efficient UCNPs ($NaYF_4$:Yb, Tm@$NaYF_4$)[18] known to date. On the other hand, the bond-dissociation energies (E_{BD}) of three known photocleavable linkers including 2-nitrobenzyl,[13,20] coumarin,[25,26] and thioether (-S-BP)[27] were calculated based on density functional theory (DFT), and the -S-BP linker with the lowest E_{BD} is selected assuming that it can be photocleaved upon a relative low intensity NIR light irradiation to trigger drug release. Finally, the thioether linker is capable of associating with *β*-cyclodextrin (*β*-CD),[28] and *β*-CD has been popularly used as a 'gatekeeper' to block pore openings and prevent drug from pre-releasing.[29] As displayed in Scheme 1A, the highly emissive UCNP is first synthesized. The UCNP is then coated with MS shell (UCMS). Furthermore, the surface of UCMS is modified with the -S-BP linker, leading to UCMS-S-BP nanoparticles. Finally, after drug Dox is loaded into the UCMS's pore channels, the pore openings are blocked through the association of -S-BP linker with *β*-CD (UCMS(Dox)-S-BP@*β*-CD). Scheme 1B shows the on-demand Dox release upon 980 nm NIR light irradiation with an ultralow intensity below MPE used, during which the upconverted UV light from UCNP cleaves the -S-BP linker leading to the disscoation of *β*-CD gatekeepers trigger on-demand Dox release.

Experimental

Materials

$YCl_3 \cdot 6H_2O$, $YbCl_3 \cdot 6H_2O$, and $TmCl_3 \cdot 6H_2O$ were bought from the JianFeng Rare Earth Company (CongHua City, People's Republic of China). Methanol, oleic acid (OA), sodium hydroxide (NaOH), cyclohexane, Hexadecyl trimethyl ammonium bromide (CTAB), tetraethyl orthosilicate (TEOS), ammonium hydroxide, N,N-Dimethylformamide (DMF), and *β*-Cyclodextrin (*β*-CD) were purchased from Sinopharm Chemical Reagent Co., Ltd. 1-Octadecene (ODE), 3-aminopropyl-triethoxysilane (APTES), 4-bromomethyl-1,1′-biphenyl (BP), 3-Mercaptopropyl-trimethoxysilane (MPTMS), and fluorescein isothiocyanate (FITC) were purchased from Aladdin. Cell counting kit-8 (CCK-8), Hoechst 33,258, fetal bovine serum (FBS) and dulbecco's modified eagle's medium (DMEM) were purchased from Sigma Aldrich (St Louis, MO, USA).

Characterization

Transmission electron microscopy (TEM) images were captured by the JEM-1400 (JEOL). UV-Vis measurement was carried out using a Cary50 UV-Vis spectrophotometer (Varian). N_2 adsorption-desorption isotherms were measured by a Micromeritics Tristar 3,000 accelerated surface area and pore size analyzer. Upconversion luminescence properties were measured in Northeast Normal University. X-ray powder diffraction (XRD) patterns were recorded by a German BRUKER D8-ADVANCE. Fluorescence microscopy images were captured by Olympus' fluorescence microscope (Japan).

Computational details of DFT

The DFT calculation was performed using the Gaussian 09 program package.[30] All the geometry optimizations were made in gas phase with Becke's three-parameter functional combined with Lee et al's correlation functional (B3LYP)[31] and 6–31+g(d,p)[32] basis sets. Furthermore,

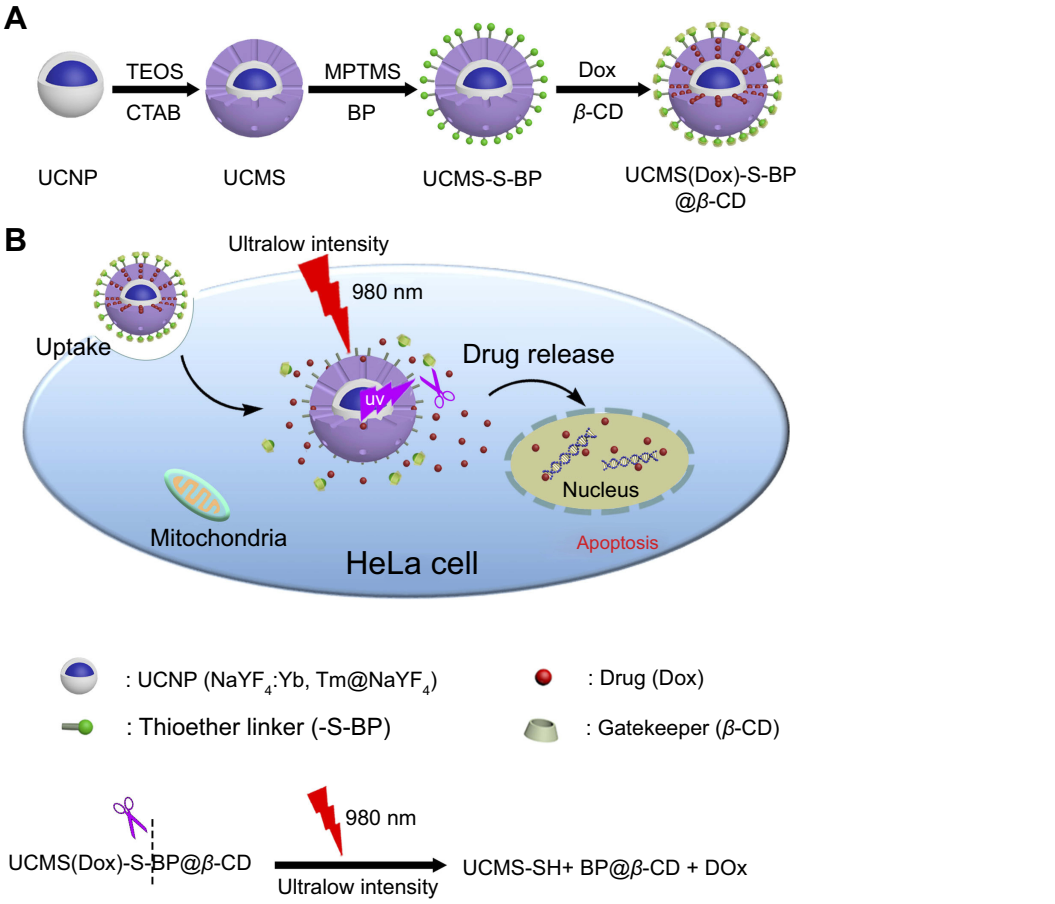

Scheme 1 Schematic illustration of an ultralow-intensity NIR light triggered on-demand drug release based on mesoporous silica-coated upconversion nanoparticles. (**A**) Synthetic procedure of UCMS(Dox)-S-BP@*β*-CD; (**B**) On-demand drug release triggered upon an ultralow-intensity (0.30 W/cm^2) NIR light irradiation by using thioether as a photolabile linker based on the as-prepared UCMS(Dox)-S-BP@*β*-CD nanoparticles. The equation for the cleavage of thioether linker is given at the bottom.

we employed the counterpoise corrections to account for basis set superposition error (BSSE).[33,34] The ball-and-stick structures of three linker molecules including thioether, coumarin and 2-nitrobenzyl (see Figure S1) were built and optimized based on Gaussian 09 program package. The E_{BD} of a molecule AB was calculated (see Table 1) by Gaussian 09 program package from the following equation:

$$E_{BD} = E_{AB} - E_A - E_B + E_{BSSE} \quad (1)$$

where E_{AB}, E_A, E_B, and E_{BSSE} are the total energy of the molecule AB, the energies of two separate fragments A and B, and error energy respectively (see Table S2). The optimized atomic coordinates of the three linker molecules are shown in Tables S3, S4 and S5, respectively.

Laser intensity measurement

The 980 nm laser intensities were measured by Thorlabs PM100D laser power meter (Thorlabs Company, Newton, NJ, USA). A fixed distance of 3 cm was set between the laser source and laser power meter. The laser intensities were recorded at different laser powers ranging from 0.10 to 2.5 W. The detailed results were given in Figure S2.

Synthesis of $NaYF_4$:Yb,Tm@$NaYF_4$ nanoparticles (UCNP)

The UCNP ($NaYF_4$:Yb,Tm@$NaYF_4$) was synthesized according to literature protocol[22] with some modifications. $YCl_3 \cdot 6H_2O$ (2.78 mmol, 843.4 mg), $YbCl_3 \cdot 6H_2O$ (1.20 mmol, 466.0 mg), and $TmCl_3 \cdot 6H_2O$ (0.02 mmol, 7.7 mg)

Table 1 The calculated E_{BD} of three linker molecules based on density functional theory using the Gaussian 09 program package

Linker	Bond	E_{BD} (KJ/mol)
Thioether	S-C	−271.2
Coumarin	O-C	−402.8
2-Nitrobenzyl	O-C	−397.2

were added to a three necked flask (250 mL) containing OA (24 mL) and ODE (60 mL). The solution was heated to 160°C and kept 3 hours under argon flow and magnetic stirring. The temperature was then cooled to 50 °C, and 40 mL of methanol containing NH_4F (16 mmol, 592.6 mg) and NaOH (10 mmol, 400.0 mg) was added. The mixture was stirred for another 30 minutes and heated to 100 °C to evaporate the methanol and then heated to 300 °C and kept 1 hour under argon protection. After it was cooled to room temperature, the product was collected by centrifugation and washed three times with ethanol/cyclohexane, and finally re-dispersed in cyclohexane (40 mL) for further use.

For the synthesis of $NaYF_4$:Yb,Tm@$NaYF_4$ nanoparticles, $YCl_3 \cdot 6H_2O$ (1.00 mmol, 303.4 mg), and pre-prepared $NaYF_4$:Yb,Tm (2.00 mmol, 20 mL) were added to a three necked flask having OA (12 mL) and ODE (30 mL). The solution was heated to 160°C and kept for 3 hours under argon protection. After the temperature was cooled to 50°C, 20 mL of methanol containing of NH_4F (4 mmol, 148.1 mg) and NaOH (2.5 mmol, 100.0 mg) was added and the mixture was stirred for another 30 minutes. Subsequently, the solution was heated to 100°C to evaporate the methanol and then heated to 300°C and kept for 1.5 hours under argon protection. The final product was dispersed in cyclohexane (20 mL) for further use.

Synthesis of MS-coated UCNP (UCMS)

The UCMS were prepared by coating UCNP with MS based on a previously reported method.[35] Briefly, the above UCNP (660 uL) in cyclohexane were added to a flask containing distilled water (20 mL) and CTAB (200 mg). The mixture was heated to 80°C and kept 30 minutes to remove cyclohexane. Then, NaOH solution (200 uL, 0.1 M) and distilled water (20 mL) were added. After 30 minutes of sonication, ethanol (2 mL) and TEOS (400 μL) were slowly added using a peristaltic pump (BT100-2J) and the mixture was stirred at 35°C for 24 hours. The nanoparticles were isolated via centrifugation (10,000 rpm, 10 minutes), washed with ethanol, and dried in a vacuum over overnight.

Synthesis of UCMS-S-BP nanoparticles

At first, the UCMS-SH nanoparticles were prepared as described in the literature,[36] except that the MS nanoparticles were replaced by UCMS. The UCMS (200 mg) and MPTMS (440 μL) were dispersed in absolute ethyl alcohol (16 mL) and sonicated for 30 minutes. The solution was stirred for 24 hours at room temperature. The resulting nanoparticles were then centrifuged (10,000 rpm, 10 minutes), washed twice with ethanol and dried under vacuum.

The UCMS-S-BP nanoparticles were prepared as described in the literature[37] with an improvement. In a 50 mL round-bottomed flask, the UCMS-SH nanoparticles (200 mg) were re-dispersed in DMF (10 mL) and sonicated for about 30 minutes. The BP (10 mg) and anhydrous K_2CO_3 (20 mg) were then added and the contents of the flask were stirred for 24 hours. After that, the products were isolated and extracted for 6 hours with NaCl (1%) in methanol to remove CTAB. The resulting UCMS-S-BP nanoparticles were collected by centrifugation (10,000 rpm, 10 minutes), washed five times with distilled water and ethanol, and dried in a vacuum.

Synthesis of FITC-UCMS-S-BP nanoparticles

The FITC-UCMS-S-BP nanoparticles were prepared as described in the literature[38] with a modification. In a 50 mL round-bottomed flask, the UCMS-S-BP nanoparticles (50 mg) were re-dispersed in ethanol (10 mL) and sonicated for about 30 minutes. Then, the APTES (30 μL) was added. The contents of the flask were stirred for another 24 hours at ambient temperature. The nanoparticles were collected by centrifugation (10,000 rpm, 10 minutes), and washed two times with DMF. The obtained nanoparticles re-dispersed in DMF and FITC (0.5 mg) were added. After 24 hours reaction, the final FITC-UCMS-S-BP nanoparticles were centrifuged (10,000 rpm, 10 minutes), washed with ethanol five times, and dried in a vacuum oven.

Loading and releasing of drug

UCMS-S-BP nanoparticles (50 mg) were first added in Dox aqueous solution (1 mg/mL, 5 mL), and treated by ultrasonic cleaner for 30 minutes. After the solution was stirred for 24 hours at room temperature, β-CD (500 mg) was added and stirred for another 24 hours. The resulting UCMS(Dox)-S-BP@β-CD nanoparticles were obtained by centrifugation (10,000 rpm, 10 minutes), and dried in a vacuum. The Dox loading efficiency was calculated to be about 3.12% (31.2 μg Dox in 1 mg UCMS-S-BP, Figure S3).

Photo-triggered Dox release experiment was done in the cuvette under dark conditions. The nanoparticles were put at the corner of a cuvette and irradiated by 980 nm NIR light at different intensities. The amount of Dox released in supernatant solutions (interval 10 minutes)

was determined by UV-Vis spectrometer. The control samples were kept in the dark without laser irradiation.

Cell culture and uptake

HeLa cells were kindly provided by Harbin Medical University Cancer Hospital (Harbin, People's Republic of China) and authenticated using short tandem repeat analysis by Genetic Testing Biotechnology Corporation (Suzhou, People's Republic of China). HeLa cells were cultured in DMEM supplemented with 1% penicillin/streptomycin and 10% FBS in an incubator (Thermo Fisher Scientific, Waltham, MA, USA).[35] For further analyses, the cells were detached by trypsin-EDTA solution (0.25%) about 1.5 minutes.

For cell uptake studies,[35,38] 1×10^4 HeLa cells per mL were seeded and incubated in 6-well cell culture cluster for 24 hours. Then, the cell medium was replaced by DMEM supplemented with FITC-UCMS-S-BP (100 μg/mL). After 4 hours incubation, the residual nanoparticles were rinsed by phosphate buffered saline (PBS). Next, the cells were fixated by formalin about 10 minutes. After that the cell nucleus were stained by Hoechst 33,258 about 30 minutes. The cell uptake images of FITC-UCMS-S-BP were observed by using a fluorescence microscope (Olympus, Japan).

Cytotoxicity of UCMS(Dox)-S-BP@β-CD nanoparticles

In vitro cytotoxicity was examined using the standard CCK-8 assay. HeLa cells (1×10^4 per well) were cultured in 96-well plates and incubated for 24 hours. The cells were then incubated with different concentration of UCMS(Dox)-S-BP@β-CD nanoparticles. After 4 hours incubation, the residual nanoparticles were rinsed, and the HeLa cells were irradiated by 980 nm NIR light at different laser intensities (0.10, 0.30 and 0.50 W/cm^2) and then incubated for 24 hours. The CCK-8 (10 μL) was added to the medium and cultured for another 2.5 hours. The microplate reader (WD-2102A) was used to test the absorbance of each well at 450 nm wavelength. The inhibition rates of cell growth were calculated by the following formula:

$$\text{Cell viability } (\%) = (A_2 - A_0/A_1 - A_0)\times100\% \quad (2)$$

where the absorbance value of blank sample A_0, control sample A_1 and treatment sample A_2 are obtained from the microplate reader (WD-2102A). The cell experiments

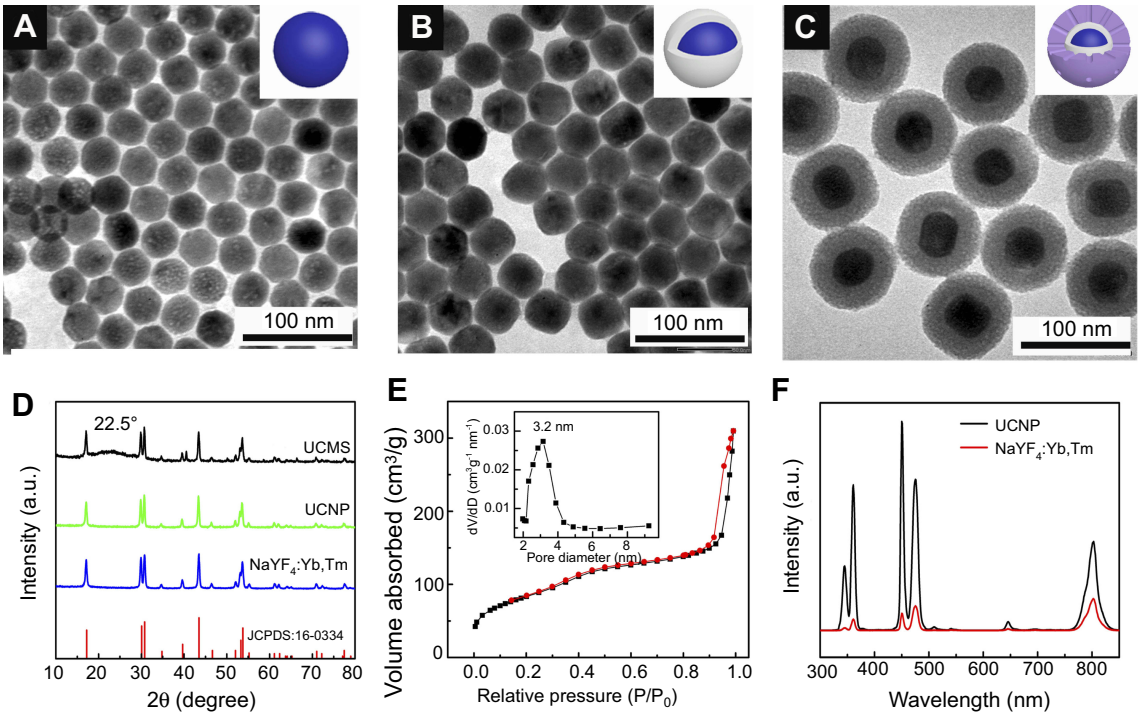

Figure 1 TEM images of (**A**) $NaYF_4$:Tm/Yb, (**B**) $NaYF_4$:Tm/Yb@$NaYF_4$ (UCNP), and (**C**) UCMS. (**D**) Powder XRD patterns of $NaYF_4$:Yb/Tm (blue), UCNP (green), and UCMS (black). The standard card of β-$NaYF_4$ (JCPDS: 16–0334) is given. (**E**) N_2 adsorption–desorption isotherm and pore size distributions (inset) of UCMS nanoparticles. (**F**) Upconversion fluorescent spectra of UCMS (black) and $NaYF_4$:Yb/Tm (red) under 980 nm NIR light irradiation.

were run three replicates in each concentration group and repeated three times.

Statistical analysis

The statistical data were shown as Mean ± SD unless otherwise noted. The statistical significance of data was tested by the T.TEST in the Microsoft Excel and a value of $P<0.05$ was considered statistically significant.

Results and discussion

Structure characterization and fluorescent measurement

As a starting point of our study, $NaYF_4$:Yb/Tm and $NaYF_4$:Yb/Tm@$NaYF_4$ nanoparticles were subsequently synthesized using a recently reported method[22] given that the resulting $NaYF_4$:Yb/Tm@$NaYF_4$ is known to be one of the most efficient UCNP. TEM images (Figure 1A and B) show they are monodispersed and uniform in size with an average diameter of 34.6±1.9 nm and 39.8±1.7 (Figure S4), respectively. The as-prepared UCNP ($NaYF_4$:Yb/Tm@$NaYF_4$) was then coated with a MS shell denoted as UCMS and the corresponding TEM image (Figure 1C) shows they have core-shell structure with an average diameter of 80.3±4.7 nm. Figure 1D shows the XRD analysis of the above-mentioned nanoparticles. It can be seen they are well-indexed as hexagonal $NaYF_4$ (all XRD peaks are in accordance with the JCPDS 16–0334 pattern) and highly crystallized which is in favor of photo-triggered biomedical application.[39] A distinct diffraction heave (2θ=22.5°) is also

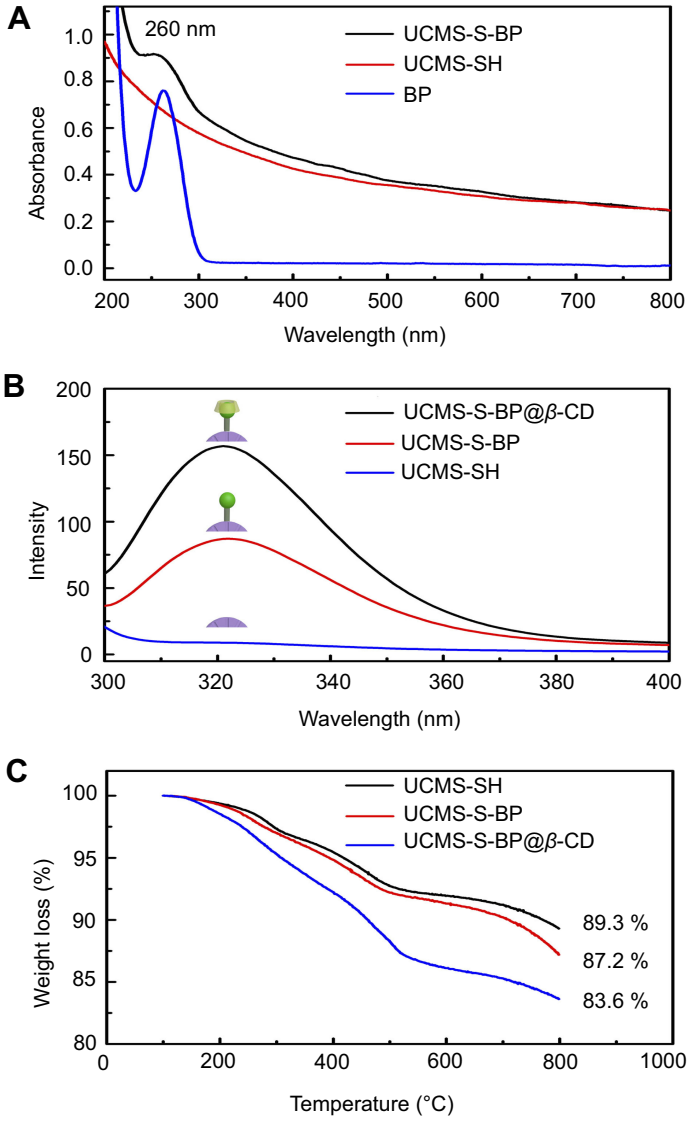

Figure 2 (**A**) UV-Vis absorption spectra of BP, UCMS-SH, and UCMS–S-BP. (**B**) Fluorescence emission spectra of UCMS, UCMS–S-BP, and UCMS-S-BP@β-CD at the same concentration (λ_{ex} =260 nm). (**C**) TGA curves of different nanoparticles: UCMS-SH, UCMS-S-BP, UCMS-S-BP@β-CD.

observed for UCMS, suggesting an amorphous MS shell is formed[13] in agreement with the previous TEM observation. Figure 1E is the nitrogen adsorption-desorption measurement of the UCMS nanoparticles, which shows the pore diameter and surface area are 3.2 nm and 301 m^2/g respectively. The fluorescent spectra measurement showed the upconversion emission intensity of UCNP is 16-fold stronger than that of naked $NaYF_4$ (Figure 1F) indicating it is highly emissive. It is therefore expected that the laser intensity required to cleave photosensitive linker and trigger drug release can be significantly reduced.

Linker selection and modification

Moreover, we also perform theoretical calculation to select a photocleavable linker with relatively low E_{BD} and expect that the intensity of NIR light for linker cleavage could be further reduced. The E_{BD} of three linker candidates including 2-nitrobenzyl, coumarin, and thioether were calculated for comparison and the results are listed in Table 1. It can be seen the E_{BD} of thioether linker (−271.2 KJ/mol) is 32% lower than that of the two others (−402.8 KJ/mol and −397.2 KJ/mol). Therefore, the thioether linker with the lowest E_{BD}, capability of associating gatekeeper β-CD, and novelty of first employment in drug release application, was selected.

The procedure for the functionalization of UCMS nanoparticles with -S-BP linker is illustrated in Figure S5 and checked by UV-Vis spectra, fluorescence emission spectra, and thermal gravimetric analysis (TGA) as shown in Figure 2. It can be seen in Figure 2A that a new absorption peak at 260 nm, which can be attributed to biphenyl portion of the -S-BP linker, is observed for the UCMS-S-BP sample in comparison with no peak observed for the UCMS sample, indicating that the -S-BP linker is successfully anchored on the MS surface. Figure 2B shows the fluorescence emission spectra of UCMS-S-BP@β-CD, UCMS-S-BP, and UCMS respectively. By comparing with UCMS showing no emission peak, the individual emission of UCMS-S-BP at 320 nm indicates that the thioether linker is successfully grafted on the surface of UCMS nanoparticles. After association of thioether linker with β-CD via host/guest interaction (β-CD capping), a further increase in intensity at 320 nm for UCMS-S-BP@β-CD is observed in agreement with the literature[40] which demonstrates a successful modification of -S-BP linker and its capability of β-CD capping. TGA measurements (Figure 2C) also showed an obvious decrease in weight of the stepwise functionalized nanoparticles, indicating a successful surface functionalization and β-CD capping.

Drug release performance

The NIR light triggered drug release behaviors of UCMS (Dox)-S-BP@β-CD nanoparticles upon NIR light irradiation at different low intensities were investigated by monitoring the change in Dox concentration with UV-Vis absorption spectroscopy. Figure 3 shows only a small amount of Dox (4.8%) is released for the control sample in 120 minutes without NIR irradiation (curve a), suggesting a satisfactory β-CD gatekeeper efficiency for our system. In contrast, Figure 3 shows about 32.4, 58.7, and 78.3% Dox are released respectively upon NIR irradiation with increasing intensity of 0.10, 0.30, and 0.50 W/cm^2

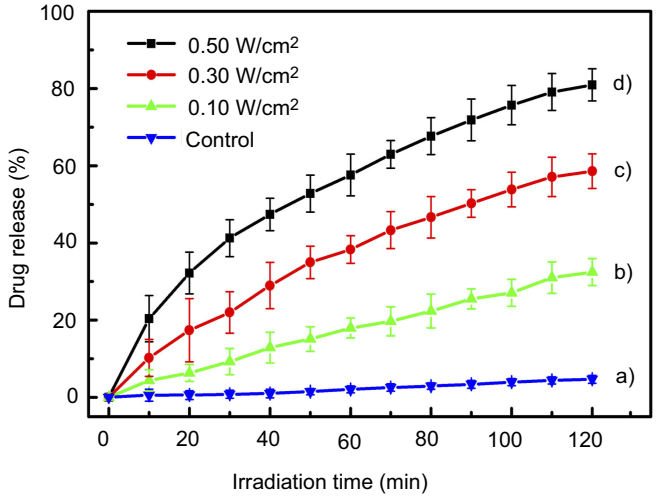

Figure 3 Dox release profiles of UCMS(Dox)-S-BP@β-CD upon 980 nm NIR light irradiation at different low intensities. The control sample was treated under dark condition without irradiation.

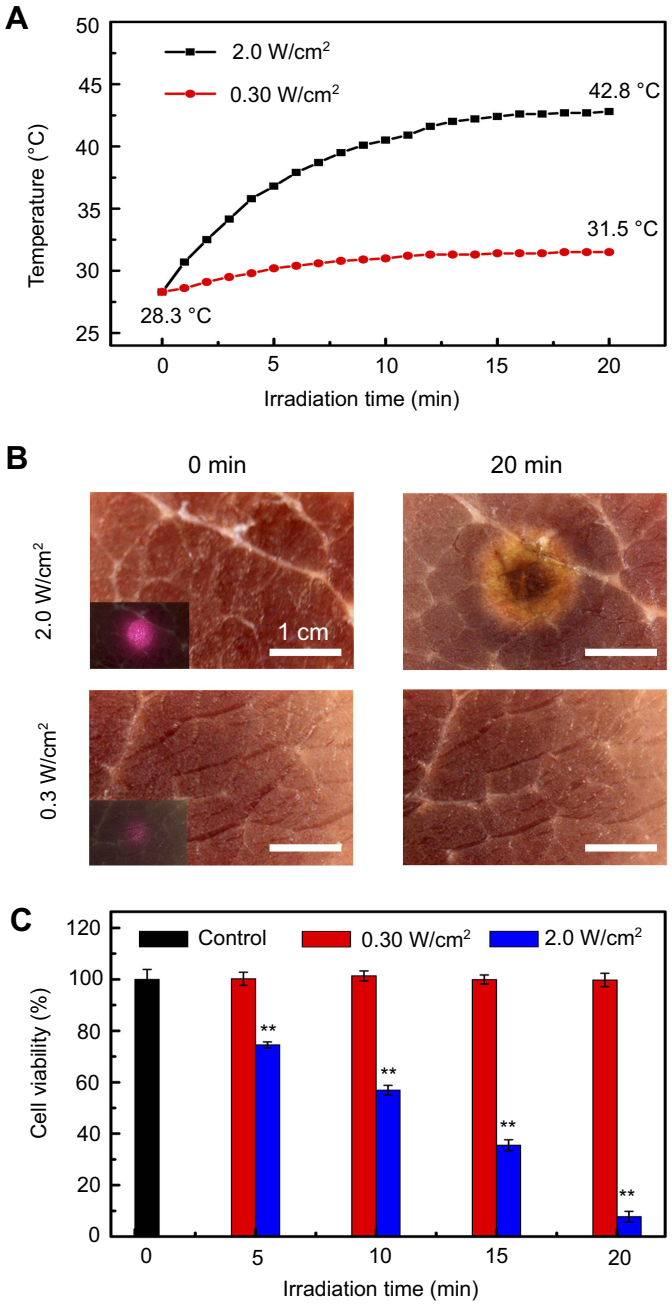

Figure 4 (**A**) Increase of water temperature upon continuous irradiation of 980 nm NIR light with intensity of 0.30 and 2.0 W/cm^2, respectively. (**B**) Photography of pork tissue before and after 980 nm light irradiation for 20 minutes with different light intensities. The scale bars represent 1 cm. (**C**) Viabilities of HeLa cells upon irradiation by 980 nm NIR light at laser intensity of 0.30 and 2.0 W/cm^2, respectively. Control: Cells cultured without laser irradiation. $^{**}P<0.01$.

(curves b–d). To meet the requirement of MPE, the excited laser intensity of 0.30 W/cm^2 was chosen as the optimum condition in the following study. The NIR light-induced cleavage of the thioether linker was also confirmed by the UV-Vis absorption spectra for a peak intensity at 260 nm, which corresponds to the cleaved biphenyl fragments of thioether linker, increases with increasing irradiation time (Figure S6). Overall, all the above results indicated ultra-low-intensity NIR light triggered on-demand drug release from UCMS(Dox)-S-BP@β-CD can be realized, in which 0.30 W/cm^2 laser intensity is lower than MPE.

Photodamage effects

The photodamage effects were investigated upon 980 nm laser irradiation with 0.30 and 2.0 W/cm^2, respectively. The NIR light-induced photothermal effects were first measured by exposure of 2 mL water in the cuvette[21] to the laser and the results are shown in Figure 4A. It can be

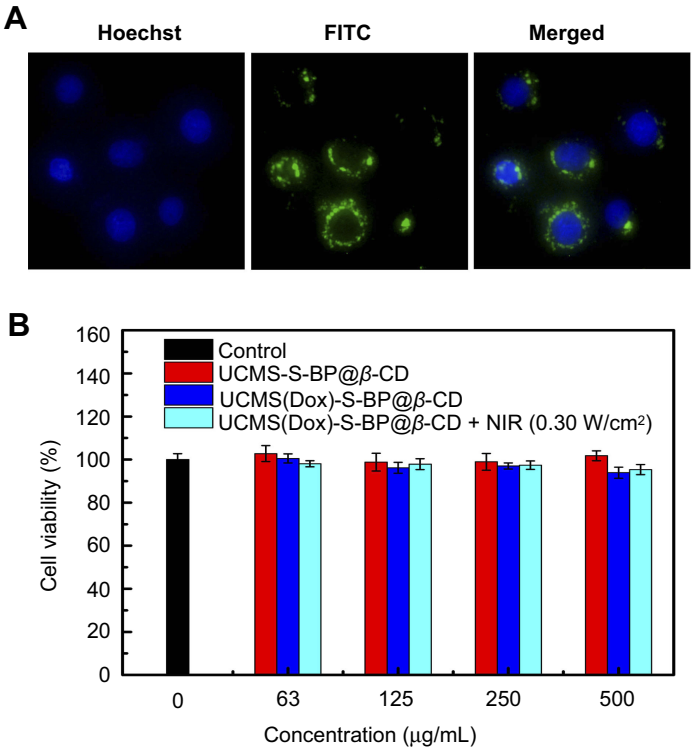

Figure 5 (**A**) Fluorescence images of HeLa cells after incubation with prepared FITC-UCMS-S-BP@*β*-CD nanocomposites for 4 hours. The nucleus and nanoparticles are dyed in blue and green, respectively. (**B**) Viabilities of HeLa cells after incubation with UCMS-S-BP@*β*-CD and UCMS(Dox)-S-BP@*β*-CD for 24 hours at different concentrations (63, 125, 250 and 500 μg/mL), respectively. Control: Cells cultured without nanoparticles and laser irradiation.

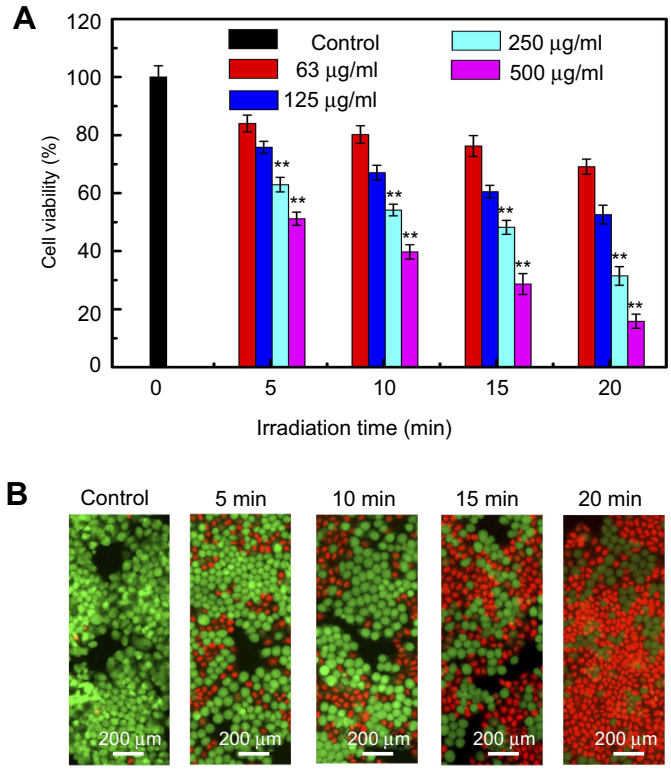

Figure 6 The viability (**A**) and fluorescence images (**B**) of HeLa cells upon 980 nm NIR light irradiation with different irradiation time (5, 10, 15 and 20 minutes). ***P*<0.01.

seen that the temperature increases with increasing irradiation time due to the high absorbance of water to 980 nm laser (Figure S7). Specifically, after 0.30 W/cm^2 laser irradiation, the water temperature slowly increases from 28.3 (room temperature) to 31.5°C in 20 minutes. In contrast, upon 2.0 W/cm^2 laser irradiation, the water temperature increases rapidly from 28.3 to 42.8°C in 20 minutes, which may "cook" normal cells to death for it is higher than the normal body temperature of 37.0°C. We next examined the practical photodamage of pork tissue for the laser irradiations at intensities of 0.30 and 2.0 W/cm^2. As shown in Figure 4B, serious burn wounds and shrinkage of pork tissue are observed after 20 minutes laser irradiation with 2.0 W/cm^2. In contrast, irradiation with ultralow laser intensity of 0.30 W/cm^2 leads to little influence on pork tissue. Finally, an in vitro cell experiment was carried out to evaluate the influence of NIR light intensity on cell viability. As displayed in Figure 4C, there is almost no negative impact on the HeLa cell viability upon 0.30 W/cm^2 laser irradiation for 20 minutes. In contrast, the cell viability upon 2.0 W/cm^2 laser irradiation deteriorates in the initial 5 minutes and almost all of the cells are killed in 20 minutes. Overall, the above results indicate that the employment of ultralow intensity of NIR light below MPE is crucial for performing safe cancer phototherapy to avoid potential overheat and photodamage on healthy neighbor cells.

In vitro cell uptake and cytotoxic effects

Cell uptake and cytotoxicity of UCMS(Dox)-S-BP@β-CD nanoparticles were first evaluated before in in-vitro experiments. For testing cell uptake, the cell nucleus were labeled by Hoechst 33,258 dye, which can combine with DNA double strands and show a bright blue fluorescence. FITC with green fluorescence was used to stain nanoparticles.[38] As shown in Figure 5A, the green fluorescence is found inside HeLa cells and mainly around the blue nuclei region, indicating the effective HeLa cell uptake of nanoparticles through either endocytosis or micropinocytosis.[8] For cytotoxicity experiment, the influence of concentration on HeLa cells viability was evaluated by CCK-8 assay. Incubation of HeLa cells with UCMS-S-BP@β-CD or the Dox loaded nanocarriers (UCMS(Dox)-S-BP@β-CD) do not cause a cell death without light irradiation (Figure 5B), indicating the loading Dox was not released form UCMS(Dox)-S-BP@β-CD in agreement with the results in Figure 3. In addition, there is also no significant cell death in the UCMS-S-BP@β-CD-treated group (95.3±2.3%) upon 980 nm irradiation, confirming the upconverted UV light can be safely used in vitro.

To verify the therapeutic effect of the UCMS(Dox)-S-BP@β-CD under ultralow intensity NIR light irradiation, the cytotoxicity was systematically evaluated by incubating HeLa cells with UCMS(Dox)-S-BP@β-CD at various concentrations. In comparison with the control sample without laser irradiation (Figure 5B), the cell viabilities upon irradiation shown in Figure 6A are significantly lower, demonstrating the cell death is caused by the released Dox from UCMS(Dox)-S-BP@β-CD. In addition, the viabilities of cells are strongly dependent on not only the nanoparticle's concentration but also irradiation time. Specifically, when the laser irradiation time increasing from 5 to 20 minutes at the maximum concentration of 500 μg/mL, the cell viabilities decrease significantly from 52.2% to 14.8%. It should be noted that a strategy of NIR light irradiation with short interval (ie,1~2.5 min) was adopted in the previous literature[18,41,42] to avoid photodamage when the high laser intensity was employed, and that according to the American National Standard for Safe Use of Laser, the intermittent exposure limit of 10 seconds is suggested for laser intensity over MPE.[24] Our ultralow intensity irradiation below MPE addresses the problem fundamentally with few restrictions on the irradiation time. The ultralow intensity irradiation can therefore make full use of its advantage both spatially and temporally to achieve the best therapeutic effect without side effects. Moreover, the fluorescence live/dead cell staining displayed similar results with the above CCK-8 assay. It can be seen in Figure 6B, HeLa cells cultured with UCMS (Dox)-S-BP@β-CD without light irradiation induced little HeLa cell death. Exposure to 980 nm laser, the mortality of HeLa cells increased with the increasing irradiation time significantly.

Conclusion

In summary, we have demonstrated a novel approach to enable ultralow-intensity NIR light triggered on-demand drug release to avoid the potential photodamage on healthy neighbor cells by employing highly emissive UCNP together with photocleavable linker with low bond dissociation energy. It was found that the selected thioether linker based on DFT calculation is cleavable for drug releasing under 980 nm NIR light irradiation with an ultralow laser intensity of 0.30 W/cm^2, which is among the lowest reported values and below the MPE of skin (0.33 W/cm^2). In vitro experiments show that about 85.2% of HeLa cells were killed within 20 minutes irradiation. We hope the

preliminary results may shed light on developing future safe photochemistry-based drug delivery systems with higher therapeutic efficiency and lower side effects.

Acknowledgments

The authors would like to acknowledge the National Natural Science Foundation of China (NSFC 51541303).

Disclosure

The authors report no conflicts of interest in this work.

References

1. Sandra McDonald MD, Philip Rubin MD, Lawrence BM. Injury to the lung from cancer therapy: clinical syndromes, measurable endpoints, and potential scoring systems. *Int J Radiat Oncol*. 1995;31(5):1187–1203. doi:10.1016/0360-3016(94)00429-O
2. Tu X, Wang L, Cao Y, et al. Efficient cancer ablation by combined photothermal and enhanced chemo-therapy based on carbon nanoparticles/doxorubicin@SiO_2 nanocomposites. *Carbon*. 2016;97:35–44. doi:10.1016/j.carbon.2015.05.043
3. Cai X, Luo Y, Yan H, et al. pH-responsive ZnO nanocluster for lung cancer chemotherapy. *ACS Appl Mater Inter*. 2017;9:5739–5747. doi:10.1021/acsami.6b13776
4. Liu S, Tian B, Wu S, et al. pH-sensitive polymer-gated multifunctional upconversion $NaYF_4$:yb/Er@$mSiO_2$ nanocomposite for oral drug delivery. *Micropor Mesopor Mat*. 2018;264:151–158. doi:10.1016/j.micromeso.2018.01.029
5. Liang X, Gao J, Jiang L, et al. Nanohybrid liposomal cerasomes with good physiological stability and rapid temperature responsiveness for high intensity focused ultrasound triggered local chemotherapy of cancer. *ACS Nano*. 2015;9(2):1280–1293. doi:10.1021/nn507282f
6. Cheng R, Tian M, Sun S, et al. Light-triggered disruption of PAG-based amphiphilic random copolymer micelles. *Langmuir*. 2015;31(28):7758–7763. doi:10.1021/acs.langmuir.5b01535
7. Fomina N, Sankaranarayanan J, Almutairi A. Photochemical mechanisms of light-triggered release from nanocarriers. *Adv Drug Deliver Rev*. 2012;64(11):1005–1020. doi:10.1016/j.addr.2012.02.006
8. Zhang Q, Liu F, Nguyen KT, et al. Multifunctional mesoporous silica nanoparticles for cancer-targeted and controlled drug delivery. *Adv Funct Mater*. 2012;22(24):5144–5156. doi:10.1002/adfm.v22.24
9. Shinmi D, Taguchi E, Iwano J, et al. One-step conjugation method for site-specific antibody–drug conjugates through reactive cysteine-engineered antibodies. *Bioconjug Chem*. 2016;27(5):1324. doi:10.1021/acs.bioconjchem.6b00417
10. Karimi M, Sahandi Zangabad P, Baghaee-Ravari S, Ghazadeh M, Mirshekari H, Hamblin MR. Smart nanostructures for cargo delivery: uncagingand activating by light. *J Am Chem Soc*. 2017;139(13):4584–4610. doi:10.1021/jacs.6b08313
11. Croissant J, Maynadier M, Gallud A, et al. Two-photon-triggered drug delivery in cancer cells using nanoimpellers. *Angew Chem Int Ed Engl*. 2013;52(51):13813–13817. doi:10.1002/anie.201308647
12. Wang YF, Liu GY, Sun LD, et al. Nd^{3+}-sensitized upconversion nanophosphors: efficient in vivo bioimaging probes with minimized heating effect. *ACS Nano*. 2013;7(8):7200–7206. doi:10.1021/nn305697q
13. Cui L, Zhang F, Wang Q, et al. NIR light responsive core–shell nanocontainers for drug delivery. *J Mater Chem B*. 2015;3(35):7046–7054. doi:10.1039/C4TB02051K
14. Wu S, Butt HJ. Near-infrared-sensitive materials based on upconverting nanoparticles. *Adv Mater*. 2016;28(6):1208–1226. doi:10.1002/adma.201502843
15. Fan W, Bu W, Shi J. On the latest three-stage development of nanomedicines based on upconversion nanoparticles. *Adv Mater*. 2016;28(21):3987–4011. doi:10.1002/adma.201505678
16. Liu J, Bu W, Pan L, Shi J. NIR-triggered anticancer drug delivery by upconverting nanoparticles with integrated azobenzene-modified mesoporous silica. *Angew Chem Int Ed Engl*. 2013;52(16):4375–4379. doi:10.1002/anie.201300183
17. Alonso-Cristobal P, Oton-Fernandez O, Mendez-Gonzalez D, et al. Synthesis, characterization, and application in hela cells of an NIR light responsive doxorubicin delivery system based on NaYF4:yb, Tm@SiO_2-PEG nanoparticles. *ACS Appl Mater Inter*. 2015;7(27):14992–14999. doi:10.1021/acsami.5b03881
18. Zhao L, Peng J, Huang Q, et al. Near-infrared photoregulated drug release in living tumor tissue via yolk-shell upconversion nanocages. *Adv Funct Mater*. 2014;24(3):363–371. doi:10.1002/adfm.201302133
19. Zhao N, Wu BY, Hu XL, et al. NIR-triggered high-efficient photodynamic and chemo-cascade therapy using caspase-3 responsive functionalized upconversion nanoparticles. *Biomaterials*. 2017;141:40–49. doi:10.1016/j.biomaterials.2017.06.031
20. Yuan YY, Min YZ, Hu QL, et al. NIR photoregulated chemo- and photodynamic cancer therapy based on conjugated polyelectrolyte-drug conjugate encapsulated upconversion nanoparticles. *Nanoscale*. 2014;6(19):11259–11272. doi:10.1039/C4NR03302G
21. Hou B, Yang W, Dong C, et al. Controlled co-release of doxorubicin and reactive oxygen species for synergistic therapy by NIR remote-triggered nanoimpellers. *Mater Sci Eng C Mater Biol Appl*. 2017;74:94–102. doi:10.1016/j.msec.2017.02.015
22. He S, Krippes K, Ritz S, et al. Ultralow-intensity near-infrared light induces drug delivery by upconverting nanoparticles. *Chem Commun (Camb)*. 2015;51(2):431–434. doi:10.1039/C4CC07489K
23. Liu G, Liu N, Zhou L, et al. NIR-responsive polypeptide copolymer upconversion composite nanoparticles for triggered drug release and enhanced cytotoxicity. *Polym Chem*. 2015;6(21):4030–4039. doi:10.1039/C5PY00479A
24. Wang D, Liu B, Quan Z, et al. New advances on the marrying of UCNPs and photothermal agents for imaging-guided diagnosis and the therapy of tumors. *J Mater Chem B*. 2017;5(12):2209–2230. doi:10.1039/C6TB03117J
25. Guardado-Alvarez TM, Sudha Devi L, Russell MM, et al. Activation of snap-top capped mesoporous silica nanocontainers using two near-infrared photons. *J Am Chem Soc*. 2013;135(38):14000–14003. doi:10.1021/ja407331n
26. Lin Q, Bao C, Cheng S, et al. Target-activated coumarin phototriggers specifically switch on fluorescence and photocleavage upon bonding to thiol-bearing protein. *J Am Chem Soc*. 2012;134(11):5052. doi:10.1021/ja300475k
27. Sucholeiki I. Solid-phase pbotochemical C-S bond cleavage of thioethers-a new approach to the solid-phase production of non-peptide molecules. *Tetrahedron*. 1994;35(40):4.
28. Arima H, Kondo T, Irie T, et al. Enhanced rectal absorption and reduced local irritation of the anti-inflammatory drug ethyl 4-biphenylylacetate in rats by complexation with water-soluble beta-cyclodextrin derivatives and formulation as oleaginous suppository. *J Pharm Sci*. 2010;81(11):1119–1125. doi:10.1002/jps.2600811116
29. Yang YW, Sun YL, Song N. Switchable host-guest systems on surfaces. *Acc Chem Res*. 2014;47(7):1950–1960. doi:10.1021/ar500022f
30. Frisch MJ, Trucks G, Schlegel HB, et al. Gaussian 09, recision B. 01. Wallingford, Gaussian Inc; 2010.
31. Becke AD. Density-functional thermochemistry. III. The role of exact exchange. *J Chem Phys*. 1993;98(7):5648–5652. doi:10.1063/1.464913
32. Francl MM, Pietro WJ, Hehre WJ, et al. Self-consistent molecular orbital methods. XXIII. A polarization-type basis set for second-row elements. *J Chem Phys*. 1982;77(7):3654–3665. doi:10.1063/1.444267
33. Boys SF, Bernardi F. The calculation of small molecular interactions by the differences of separate total energies. Some procedures with reduced errors. *Mol Phys*. 2006;19(4):553–566. doi:10.1080/00268977000101561

34. Schwenke DW, Truhlar DG. Systematic study of basis set superposition errors in the calculated interaction energy of two HF molecules. *J Chem Phys*. 1985;82(5):2418–2426. doi:10.1063/1.448335
35. Han R, Shi J, Liu Z, Wang H, Wang Y. Fabrication of mesoporous-silica-coated upconverting nanoparticles with ultrafast photosensitizer loading and 808 nm NIR-light-triggering capability for photodynamic therapy. *Chem Asian J*. 2017;12(17). doi:10.1002/asia.201700836
36. Zhang J, Yuan ZF, Wang Y, et al. Multifunctional envelope-type mesoporous silica nanoparticles for tumor-triggered targeting drug delivery. *J Am Chem Soc*. 2013;135(13):5068–5073. doi:10.1021/ja312004m
37. Khurana JM, Sahoo PK. Chemoselective alkylation of thiols: a detailed investigation of reactions of thiols with halides. *Synthetic Commun*. 1992;22(12):1691–1702. doi:10.1080/00397919208020489
38. Li X, Xie QR, Zhang J, et al. The packaging of siRNA within the mesoporous structure of silica nanoparticles. *Biomaterials*. 2011;32(35):9546–9556. doi:10.1016/j.biomaterials.2011.08.068
39. Chen X, Peng D, Ju Q, et al. Photon upconversion in core-shell nanoparticles. *Chem Soc Rev*. 2015;44(6):1318–1330. doi:10.1039/C4CS00151F
40. Liu Z, Shi J, Han R, Wang H. Competitive-binding activated supramolecular nanovalves based on *β*-Cyclodextrin complexes. *ChemistrySelect*. 2017;2(19):5341–5347. doi:10.1002/slct.201700956
41. Wen L, Jiasi W, Jinsong R, et al. Near-infrared upconversion controls photocaged cell adhesion. *J Am Chem Soc*. 2014;136(6):2248–2251. doi:10.1021/ja412364m
42. Yue C, Zhang C, Alfranca G, et al. Near-infrared light triggered ROS-activated theranostic platform based on Ce6-CPT-UCNPs for simultaneous fluorescence imaging and chemo-photodynamic combined therapy. *Theranostics*. 2016;6(4):456–469. doi:10.7150/thno.14101